Vertical temperature gradients

In an effort to further diminish any possible temperature inaccuracies, the vertical gradient across the silicon chip was also experimentally evaluated with the external Pt100 sensor and the 2700 Multi-meter Data Acquisition System. Temperature was directly read on a particular spot of the Peltier cell surface and then read again at the same spot across a bare 300 μm silicon chip. The results, consistent with computer simulations (see p.221), indicated that the maximum thermal gradient across the silicon chip was in the whereabouts of ±0.1-0.2 ºC.

Optimization

Peltier operational range

As discussed previously (see p.149), the obvious solution to the limitations of the Peltier cell operation ranges was the ordering of a custom multistage Peltier cell, but, since this was a costly solution, both in terms of time and money, it was decided first to try some feasible alternatives.

Double Peltier assemblies

A first intuitive notion was to emulate the properties of a multistage Peltier cell by gluing together two independent cells. Since all commercial multistage series display a pyramidal shape to attain a better heat dissipation coefficient, the same approach was followed here. Assays were made gluing together the available Peltier cells (a 33W 30x30 mm^2 cell on top of a and a 68W, 40x40 mm^2 cell). The cells were bonded together with 340 Heatsink compound (*Dow Corning*) and their operational response was studied under different electrical configurations (serial and parallel connection). The results are shown in Figure 85.

As it can be seen in Figure 85, the results were clearly unsatisfactory. Although the double (33W-68W) parallel Peltier configuration yielded faster transient times from 50 to 95 ºC, they were not exceedingly faster than those of the single 68W Peltier cell alone and still did not fit the necessary requirements for fast thermocycling. Moreover, the superior rising times of the double-parallel Peltier configuration were achieved at the cost of substantially rising the power consumption of the system and were also negatively compensated by fall speeds slightly slower than those of the

single 68W Peltier. This lack of efficiency is better illustrated by the serial connection of the two Peltier cells, which produced far worse results than those of the single 68W cell, and can be partly explained due the thermal gradient imposed by the inefficient junction of the two Peltier cells ceramic cappings.

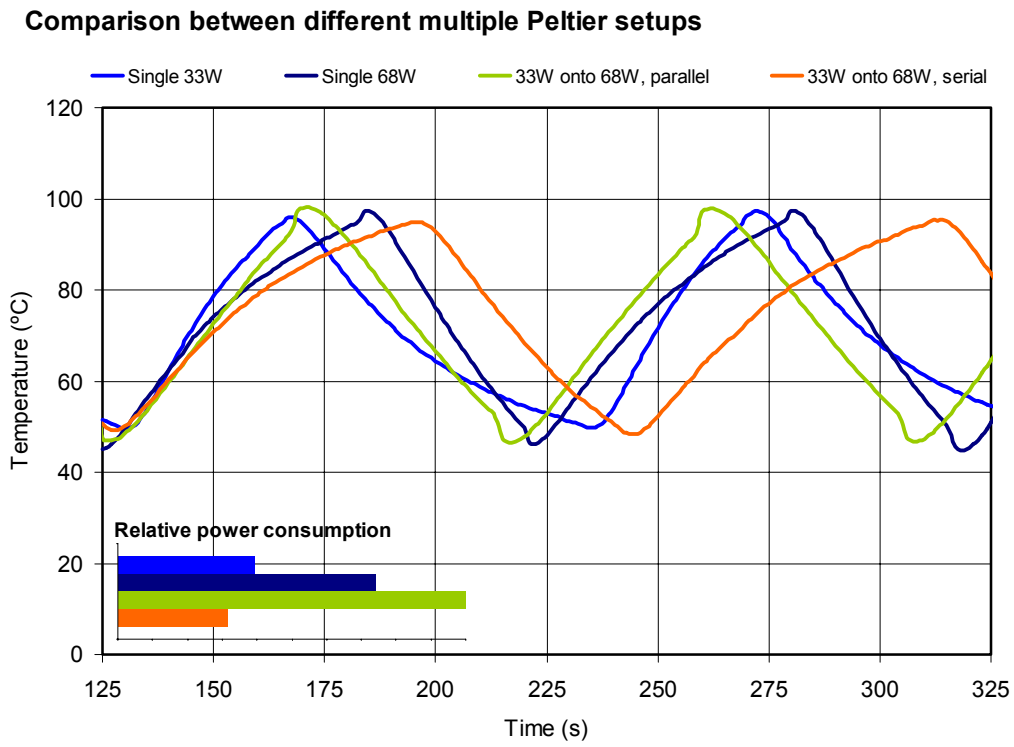

Figure 85 - Comparison of different Peltier setups and interconnections.

Forced ambient temperature

Seeing that the superimposing of Peltier cells did not yield the desired results, a simpler provisional solution (which was later to become definitive) was devised. Since Peltier cells establish a current-dependent temperature differential across their hot and cold surfaces, a new setup was concocted in which the heat dissipater lay on a Series 1000 laboratory hot-plate stirrer (*Jenway*), see Figure 86. With this new setup, experiments were carried out to assess whether it could provide the desired transient times for fast PCR operation. Using the hot-plate as a thermostat-controlled heating element, the temperature of the heat dissipater surface was set to 40-60 °C and monitored with the surface thermocouple. As it can be gauged by looking at Figure 87, the results for fast thermocycling parameters were strikingly better than those obtained with the previous setup.

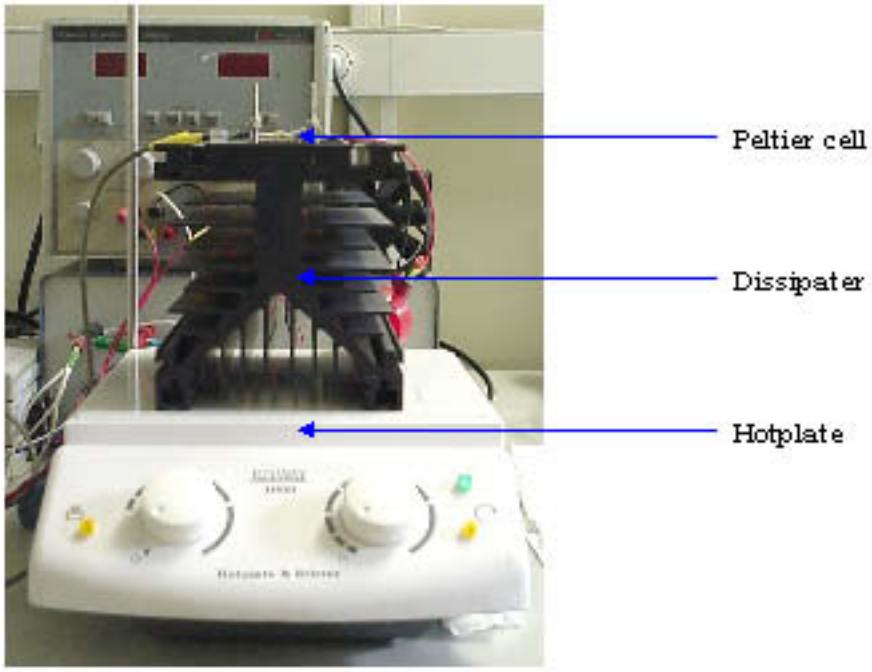

Figure 86 - Forced-ambient cold side temperature with a hotplate-stirrer.

With the new setup, 72 to 95 °C transition times were reduced to 6 s (4 °C/s), while fall transients remained still fast enough (about 5 °C/s) for robust PCR operation and, hence, the hot-plate setup was considered a neat temporary solution to the problem of Peltier cell operational range.

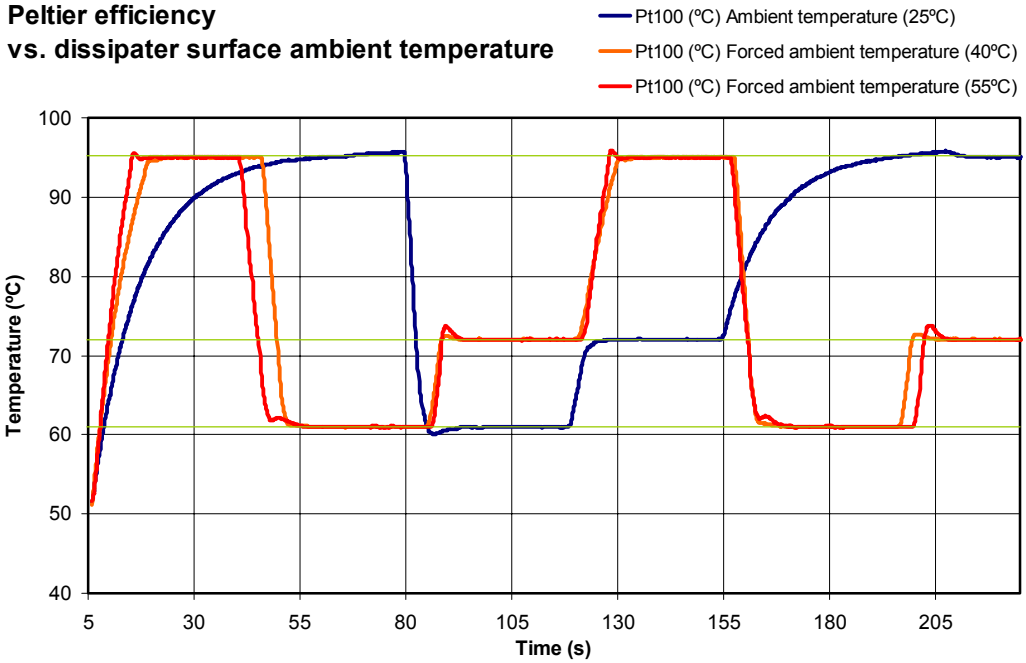

Figure 87 - Thermocycling results with forced dissipater surface temperature (40-60 °C). Overshooting in the 55 °C experiment is caused by an inaccurate setting of the PID parameters and was successfully removed in further experiments.

Temperature accuracy

Since, due to the nature of the own Peltier cells, the previously observed non-uniformities on the surface of the cell were unavoidable, custom free-oxygen copper blocks were cut to fit Peltier cell dimensions and allow an efficient and homogenous distribution of temperature across their surfaces. Two different copper blocks 40x40x1 mm^3 and 40x40x2 mm^3 were fabricated and bonded to the Peltier cell hot surface with 340 Heat-Sink compound (*Dow Corning*) in order to evaluate their effects on temperature distribution and transient times.

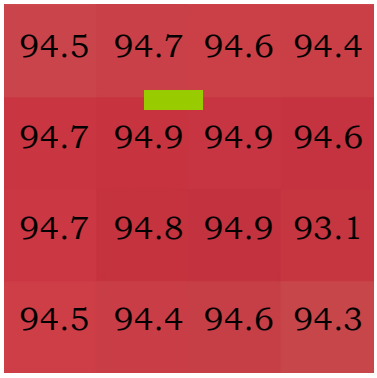

Figure 88 - Temperature distribution on a 1 mm-thick copper block surface as measured with the external Pt100 sensor. The green rectangle represents the position of the PID-control Pt100.

Temperature distribution on the surface of 1 mm and 2 mm copper blocks was greatly enhanced with respect to temperature distribution on the bare Peltier cell surface (see Figure 88). The maximum temperature gradients observed across the block were not superior to 0.5 ºC (well within the tolerance range of conventional PCR thermocyclers), and they were not much improved by the use of 2 mm copper blocks, decreasing only to about 0.4 ºC. Hence, noting that the difference in temperature homogeneity did not vary greatly between 1 mm and 2 mm-thick copper blocks, the transient behavior of the system using both kinds of blocks was then assessed.

The results for 1 mm and 2 mm-thick copper blocks (see Figure 89) suggested that transient rates were excessively lowered with 2 mm blocks. Even if PID parameters were accurately adjusted, the increased thermal mass of 2 mm blocks implied a compromise between system stability (avoiding overshooting) and transient response. Hence, 1 mm blocks were considered the best solution for redistributing temperature across the system surface without loosing much transient response.

Transient behavior with copper blocks

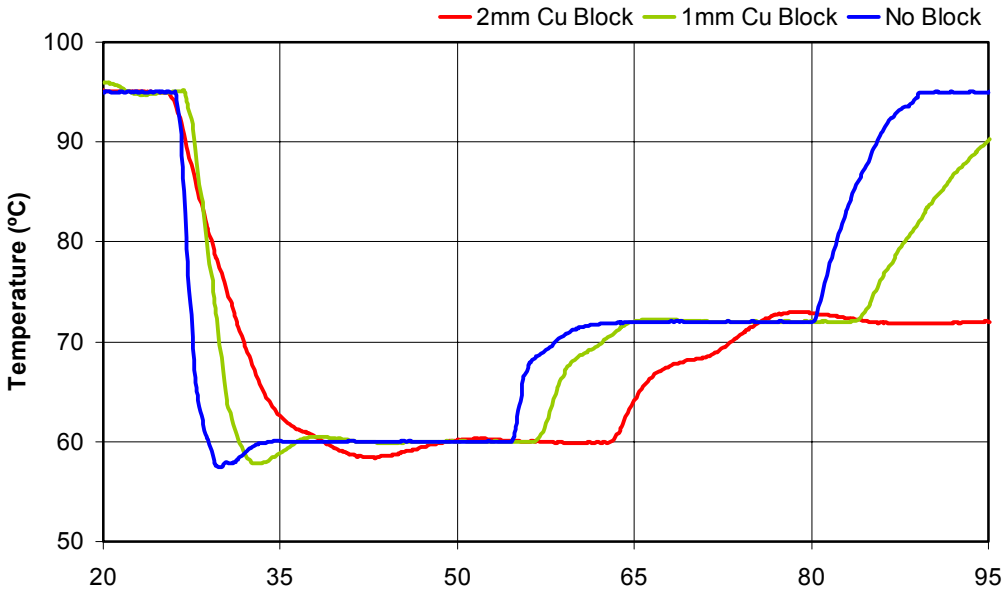

Figure 89 - Degraded transient behavior due to the added thermal mass of the thermal blocks. Measurements were made in standard ambient temperature (~25 ºC) conditions. Overshooting in temperature control is due to inaccurate setting of the PID parameters.

To avoid any further temperature inaccuracies due to the vertical thermal gradients across the silicon and to inefficient heat distribution across the silicon chips, the system was thermally characterized using a 1 mm-thick copper block and a 40x10x0.3 mm^3 silicon chip as a base for clamping of the PID-control Pt100 device. The base silicon chip was positioned at 8 mm from the Peltier cell border and glued to the copper block with 340 Heat-Sink compound (*Dow Corning*). With this setup (see Figure 90), temperature on the surface of a fake 40x10x0.3 mm^3 PCR-chip was monitored with the external Pt100 device.

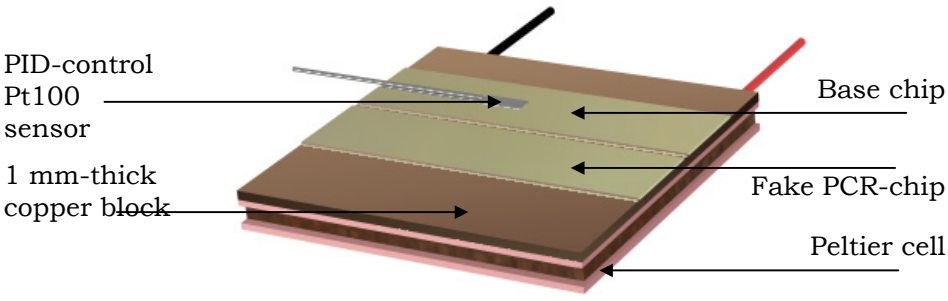

Figure 90 - Setup for experimental characterization of temperature gradients on a fake PCR-chip.

The results (see Figure 91) indicated that the maximum temperature deviations across the fake PCR-chip surface were below -0.2 °C and that the difference between the PID-control set temperature and that at the center of the fake PCR-chip was a reliable ±0.1 °C, yielding a highly precise temperature control, with fast transient times (using forced ambient temperature), as shown in Figure 92.

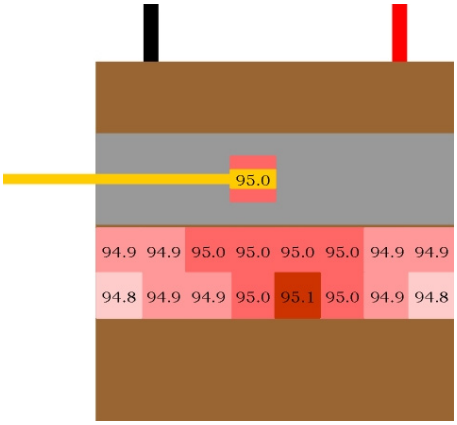

Figure 91 - Experimental characterization of the temperature gradient across a fake PCR-chip surface for a set temperature of 95 °C. Measurements were mainly carried out at 95 °C (the most problematic temperature, due to convection effects), but were also cross-checked at other typical PCR temperatures (72 and 61 °C, data not shown), yielding similar results.

Fast and accurate temperature control

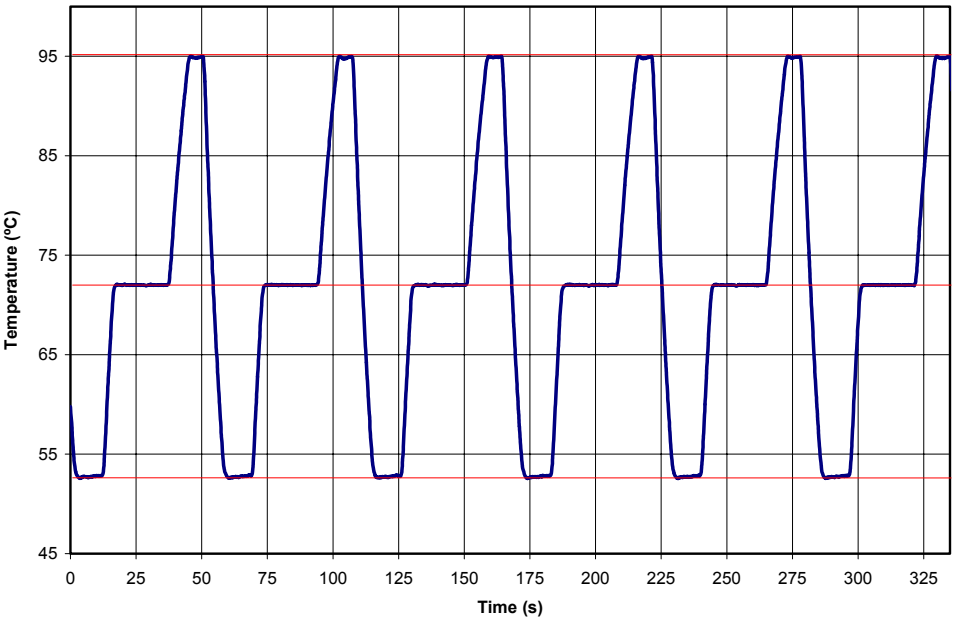

Figure 92 - Reliable temperature control displaying fast transients and quick and accurate stabilization without overshooting. Data from a PCR experiment with a forced ambient temperature of 45 °C and the following cycling parameters: 95 °C - 5 s / 53 °C - 10 s / 72 °C - 20 s. Average transient: rise - 4 °C/s, fall - 5 °C/s.

Results such as those of Figure 92 were considered markedly satisfactory and robust enough to guarantee that any contingencies bearing on the results of PCR amplification assays with PCR-chips were not originating from an improper temperature control.

4.5. CAPPING STRATEGIES

Although capping strategies conform an integral part of the development of the external fast thermocycler, they are discussed apart because, due their own special characteristics, they did generate a nearly independent case study. As it has been previously noted (see p.100 and p.126), capping strategies have not been widely discussed in the literature. Nevertheless, in the special case of silicon chips with back-etched access holes, capping issues are not an straightforward matter due to several reasons. For one, capping materials may be a source of PCR inhibitors or may, after several assays, contaminate the chip reservoir surface. Moreover, in back-etched chips, the capping film or gasket can pose a thermal barrier between the heating element and the chip, yielding non-reproducible results. The following is an sketchy account of the different capping strategies evaluated during and after development of the external fast thermocycler, and of the problems and advantages caused by each of them.

4.5.1. ACRYLIC TAPE CAPPING

A standard capping technique reported in the literature is the use of an acrylic tape for effectively sealing the PCR device during amplification ([Taylor1997], [Lin2000a], [Zhan2000]). In their more detailed article, the acrylic tape proposed by *Taylor's* team is the biocompatible ARCare 7759 0.5 mm-thick film (*Adhesives Research*). Following their lead, a sample of the film was ordered from *Adhesives Research* and different studies were carried out to assess its PCR-friendliness and its implications on thermal transfer and chip unloading methodologies.

PCR compatibility

ARCare7759 (*Adhesives Reseach*) is a biocompatible polymeric tape that has been reported as PCR compatible. Nonetheless, at the time of this research, the only evidence supporting such biocompatibility came from a

single research group and, after some unsuccessful PCR assays, a battery of experiments was devised to test their hypothesis.

Standard PCR experiments with ARCare7759 were kindly carried out by Nadina Erill at the BioPAT service of the Hospital de Barcelona. A 185 bp fragment of the human p53 exon #7 was PCR amplified using the following conditions:

Quantity	**Reagent**
18.2 µl	milliQ H_2O
2.5 µl	10x $MgCl_2$ Buffer
2 µl	10 nM dNTPs
0.5 µl	10 µM sense primer
0.5 µl	10 µM antisense primer
0.3 µl	3.5 U/µl Expand™ High Fidelity System (*Boehringer Mannheim Corp.*)
1 µl	200 ng/µl sample DNA

Cycling protocol:

94 °C - 5 min
94 °C - 30 s \
61 °C - 30 s x30
72 °C - 30 s /
72 °C - 7 min
4 °C - ∞

Table 3 - PCR protocols for ARCare PCR-compatibility experiments.

Normal eppendorf tubes were used as positive controls, while test tubes contained normal (closed) and torn open (open) ARCare7759 film in contact with the PCR sample.

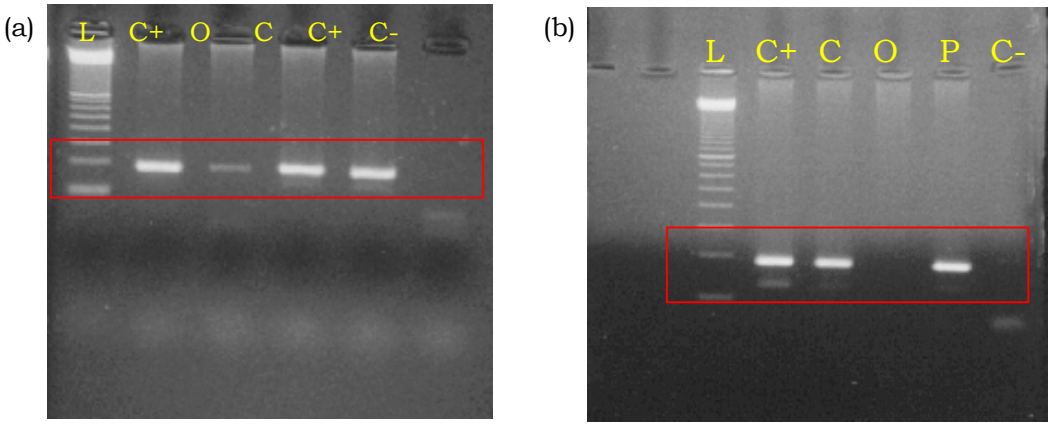

Figure 93 - PCR experiments with ARCare7759 acrylic tape. A ~1 mm^2 tape fragment was inserted in standard eppendorf tubes, making contact with p53 exon #7 amplification mix. The L lane corresponds to the DNA ladder, while C+ lanes represent experiments without tape and C- ones correspond to negative control tubes. O and C lanes mark, respectively, experiments with torn open and closed ARCare7759 tape. In experiment (a), the tape was in partial contact with the PCR solution, while in experiment (b), showing complete inhibition of PCR, the tape was fully immersed into the PCR solution.

Repeated trials (see Figure 93) indicated that the presence of torn open (O) ARCare7759 tape induced partial or complete inhibition of the PCR reaction (depending on the area of tape exposure), while closed ARCare7759 tape (C) did not interfere with PCR.

Thermal transfer and reagent extraction

Although discouraging, the compatibility results of acrylic tape did not completely preclude its use in PCR-chips. As already seen (see p.145), the formation of air bubbles at PCR-chip orifices was almost unavoidable, and the presence of such a thin air layer could theoretically prevent the PCR sample from making contact with the inhibiting acrylic tape surface (as derived from the commentaries of *Zhan et al.* [Zhan2000]). Nevertheless, even in such likelihood, the use of acrylic tapes posed other physical problems in the basic scheme of the external thermocycler here developed.

Thermal transfer

Although ARCare7759 is a thin film tape, its thickness (0.5 mm) and nature introduce a thermal gradient in the experimental setup of the external thermocycler. This is an acute problem when dealing with back-etched chips, in which the thermally conducting side (silicon) is the same in which the access holes have been opened (and thus must be capped). In this case, there are to logical alternatives for sealing the device with an acrylic tape (see Figure 94).

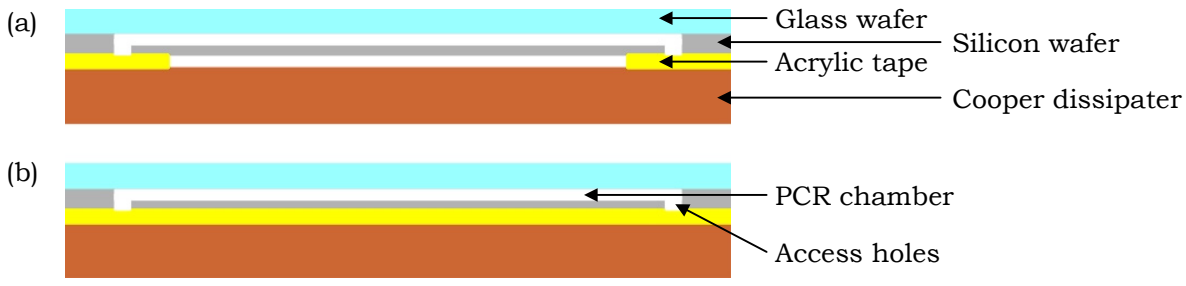

Figure 94 - Different sealing strategies with acrylic tape, covering (a) hole regions and leaving an air layer below the PCR chamber or (b) the whole PCR-chip.

The first, and most intuitive, alternative is to use two short patches of tape to seal the hole regions of the chip (see Figure 94a). Nonetheless, this leaves

the middle part of the chip (and the corresponding major area of the PCR-chamber) physically separated from the heat source and, hence, it requires that a thermally conducting layer (such as 340 heat-sink compound (*Dow Corning*) or mineral oil) be placed below the chip, an option that, due to evaporation and non-homogeneity issues, is not very reliable. Otherwise, the whole chip may be sealed with acrylic tape (see Figure 94b), thus creating a homogenous tape layer. This option is somehow more reliable, since the tape layer is, at least theoretically, homogenous. The idea was put into practice and the thermal gradient of the acrylic tape was evaluated with an independent Pt100 sensor, using a scheme similar to that of previous temperature characterizations (see p.175). The experimental results suggested that the vertical thermal gradient imposed by the acrylic tape was in the whereabouts of 0.5 ºC for a set temperature of 95 ºC, but they also uncovered non-homogeneities in the temperature distribution across the chip surface, making the estimated gradient unreliable. When investigated, these in-homogeneities were seen to arise from small air bubbles that had originated (and were difficult to avoid) on the back surface of the chip during tape sealing. These bubbles expanded with the applied heat and physically separated the chip from the underlying copper block, provoking differential temperature gradients that were reflected at the opposite surface.

Reagent extraction

A final, but not trivial, problem stemming from the use of acrylic tape sealing was the recurrent breakage of chip membranes during the removal of the tape layer previous to reagent extraction. ARCare7759 creates a strong bond with oxide-passivated silicon and it is difficult to remove with standard lateral stresses. Although organic solvents could have been used to remove the tape, their use was not recommended due to their more than probable interaction with PCR products. In their experimentation, *Taylor's* team used 0.5 mm silicon wafers with more robust membranes, and this probably permitted a reliable removal of the acrylic tape layer without membrane breakage. However, with the 300 µm-thick silicon wafers here used, the possibility of membrane breakage could not be discarded when using tape patches, and was almost ensured when the tape covered the whole back side of the chip.